

more stable. The need for the study of more octahedral complexes of differing steric requirements and containing metals in differing oxidation states is clear.

Acknowledgment.—The author is grateful to the

donors of the Petroleum Research Fund, administered by the American Chemical Society, for partial support of this work. He is also indebted to Mr. Leon A. Epps for supplying the complexes and to Professor John L. Burmeister for helpful discussions.

CONTRIBUTION FROM THE DEPARTMENT OF CHEMISTRY,
UNIVERSITY OF MASSACHUSETTS, AMHERST, MASSACHUSETTS 01002

Pentacoordinated Molecules. XVII.¹ Molecular Structure of HPF_4 and H_2PF_3 in the Gas, Liquid, and Solid States from Infrared and Laser Raman Spectroscopy

BY ROBERT R. HOLMES* AND CHARLES J. HORA, JR.

Received December 22, 1971

The vapor-phase and solid-state infrared spectra ($4000\text{--}33\text{ cm}^{-1}$) of HPF_4 and H_2PF_3 are reported along with laser Raman spectra for these substances in the liquid and solid states. Polarization measurements were obtained on the liquid states. Complete analysis of the vibrational data supports the trigonal-bipyramidal conformation for the vapor state with the protons residing in equatorial sites for both HPF_4 and H_2PF_3 . In contrast to earlier literature on H_2PF_3 , the data further suggest retention of the gas-phase structure in the liquid and solid states. The same holds true for HPF_4 . With the aid of band-shape analysis on the highly structured infrared spectra, detailed spectral assignments are made supporting the C_{2v} point group. Intramolecular exchange mechanisms consistent with the vibrational assignments are presented.

Introduction

A microwave study of HPF_4 ² has established its vapor-state structure as a trigonal bipyramid with an equatorially positioned proton. This is consistent with a similar structure established for CH_3PF_4 by electron diffraction³ and other monosubstituted derivatives of PF_5 indicated by vibrational analysis to have this conformation with the unique ligand in an equatorial site. These derivatives are CCl_3PF_4 ,^{4a} $(\text{CH}_3)_3\text{CPF}_4$,^{4b} CF_3PF_4 ,⁵ CIPF_4 ,⁶ and CH_3PF_4 .⁷

An infrared and Raman study of H_2PF_3 ^{8,9} suggested a trigonal bipyramid for the vapor with the hydrogen atoms again in equatorial sites as expected. However, association to a fluorine bridge dimer was reported⁹ to occur in the liquid and solid states.

In contrast to these results, ^{19}F nmr data¹⁰ for the liquid at -46° are consistent with the structure reported for the vapor. Because of the difficulties in handling^{8,10} these highly reactive species, reproducible nmr spectra were not easy to obtain. Broad fluorine resonances in the intensity ratio of about 2:1 were observed¹⁰ having a doublet character (P-F spin coupling). On the other hand the ^1H and ^{31}P splitting patterns were consistent with the presence of three equiv-

alent fluorine atoms and, hence, indicative of the presence of intramolecular exchange at low temperature. At higher temperatures (-15°), the ^{19}F pattern¹⁰ also pointed to the onset of positional exchange.

In view of the discrepancies between the vibrational interpretation⁹ and the nmr findings,¹⁰ a more detailed study of the structure of H_2PF_3 was undertaken by infrared and laser Raman spectroscopy. In addition, clarification of the condensed-state structure is needed in order to properly interpret intramolecular exchange phenomena observed¹⁰ here. As with H_2PF_3 , HPF_4 has been studied previously;^{8,10} however, no definitive vibrational analysis has been carried out. To ascertain if HPF_4 behaved analogously and as an aid in assignments, its spectra were also investigated in the gas, liquid, and solid states.

Experimental Section

Materials.—Both HPF_4 and H_2PF_3 were prepared as before⁸ from the reaction of hydrogen fluoride with the respective phosphorous acid in a copper vacuum system containing Kel-F U traps. The products were purified by trap-to-trap distillation. The starting materials, anhydrous hydrogen fluoride (Matheson, 99.9%) and phosphorous acid (Fisher Certified reagent, 98.9%), were used without further purification. Hypophosphorous acid (Fisher, purified) needed for the preparation of H_2PF_3 was purified as described previously.⁸

Since the compounds are highly reactive with Pyrex and quartz, H_2PF_3 more so than HPF_4 , subsequent handling for spectral determinations made use of glass-free systems. Samples were fractionated just prior to use. During the course of any of the spectral measurements, no changes in band intensities were observed. It was determined that samples of HPF_4 contained in Monel infrared cells partially decomposed into HF and PF_3 during a 24-hr period. The latter were detected from their characteristic infrared spectra. The samples could be stored at -78° in Kel-F, stainless steel, or Monel ampoules for prolonged periods with no noticeable decomposition.

Spectral Measurements.—Infrared spectra were recorded with a Beckman IR 11-12 spectrophotometer. In all runs the instrument was purged with dry nitrogen. The far-infrared region was calibrated with HF, HCl, and H_2O vapor. The higher region was calibrated with CO_2 and H_2O vapor. Samples for gas-phase

(1) Presented in part at the Symposium on Raman Applications in Inorganic Chemistry, Division of Inorganic Chemistry, 163rd National Meeting of the American Chemical Society, Boston, Mass., April 1972. Previous paper: R. R. Holmes and M. Fild, *Inorg. Chem.*, **10**, 1109 (1971).

(2) S. B. Pierce and C. D. Cornwell, *J. Chem. Phys.*, **48**, 2118 (1968).

(3) L. S. Bartell and K. W. Hansen, *Inorg. Chem.*, **4**, 1777 (1965).

(4) (a) R. R. Holmes and M. Fild, *J. Chem. Phys.*, **53**, 4161 (1970); (b) *Inorg. Chem.*, **10**, 1109 (1971).

(5) (a) J. E. Griffiths, *J. Chem. Phys.*, **49**, 1307 (1968). (b) In the case of CF_3PF_4 , however, an incomplete microwave study suggests a symmetric top with the CF_3 group in an axial position: E. A. Cohen and C. D. Cornwell, *Inorg. Chem.*, **7**, 398 (1968).

(6) R. R. Holmes, *J. Chem. Phys.*, **46**, 3718 (1967).

(7) A. J. Downs and R. Schmutzler, *Spectrochim. Acta*, **21**, 1927 (1965).

(8) R. R. Holmes and R. N. Storey, *Inorg. Chem.*, **5**, 2146 (1966).

(9) J. Goubeau, R. Baumgärtner, and H. Weiss, *Z. Anorg. Allg. Chem.*, **348**, 286 (1966).

(10) P. M. Treichel, R. A. Goodrich, and S. B. Pierce, *J. Amer. Chem. Soc.*, **89**, 2017 (1967).

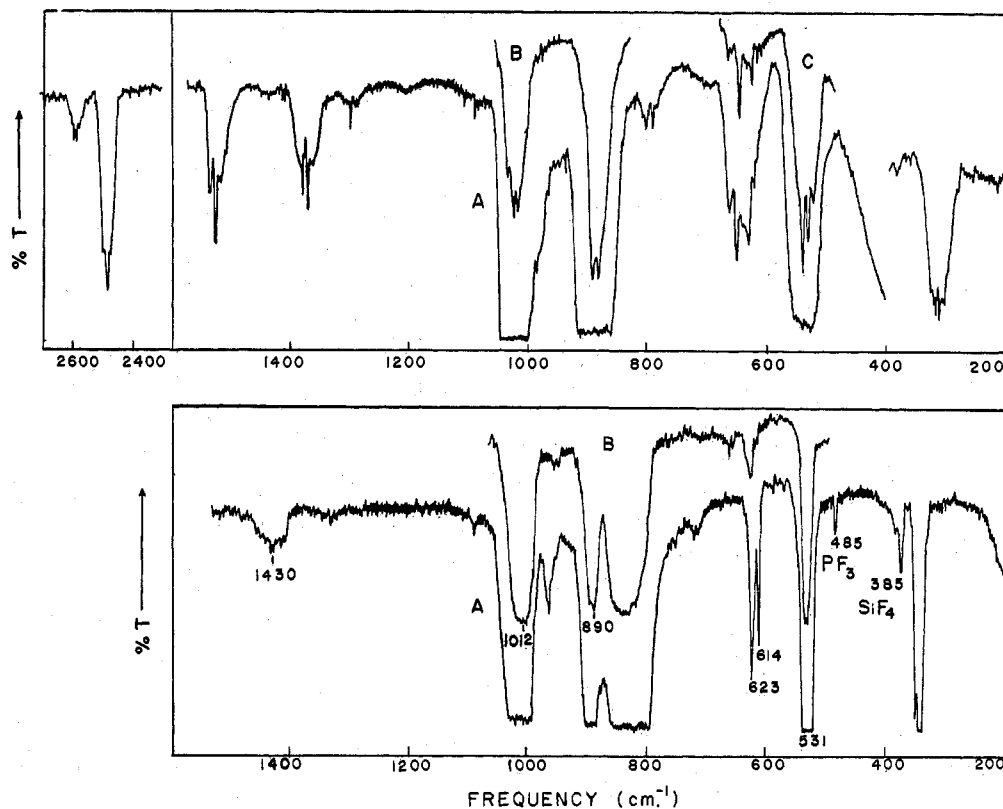


Figure 1.—Infrared spectrum of HPF_4 . Top, vapor state at 25° : (A) $l = 10$ cm, (B) $l = 0.5$ cm, (C) $l = 1.2$ cm; $l = 10$ cm, AgCl windows, 400 – 2700 cm^{-1} , polyethylene windows, 200 – 400 cm^{-1} . Bottom, solid film at -190° : (A) medium thickness, (B) low thickness, CsI window.

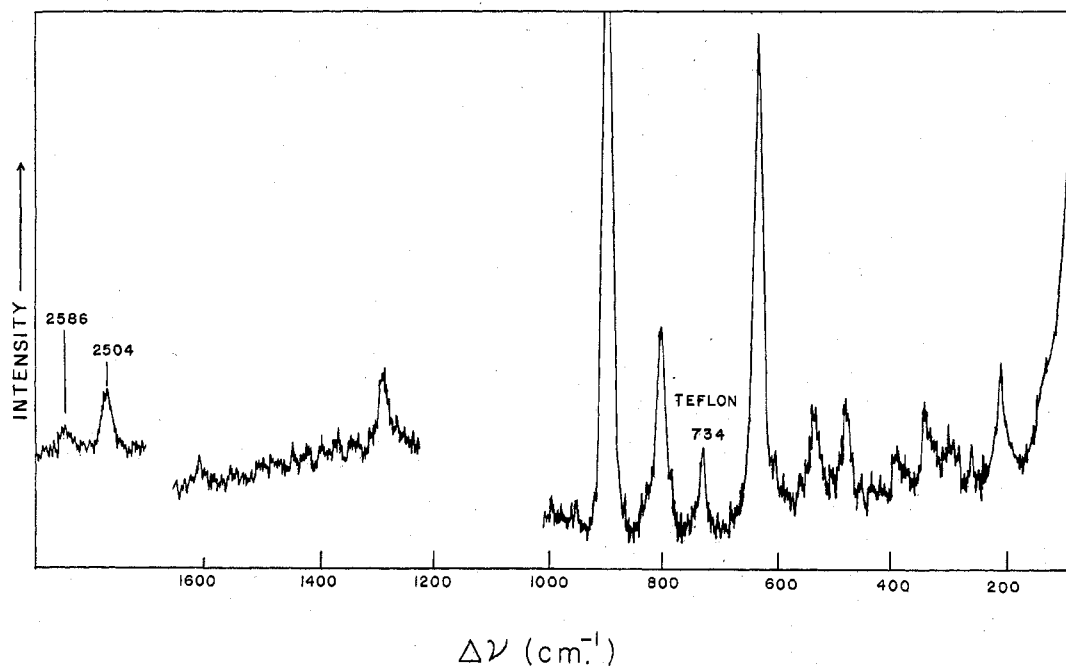


Figure 2.—Raman spectrum of liquid HPF_4 at -63° .

analysis were contained in 10-cm Monel metal cells fitted with high-density polyethylene windows for the 33 – 600 - cm^{-1} region and with AgCl windows for the 400 – 4000 - cm^{-1} region.

Low-temperature gas-phase studies employed a Plexiglas housing for the Monel metal cell placed in the infrared beam. Precooled nitrogen gas was circulated within the housing to obtain the desired temperature. The temperature was measured

by means of a copper–constantan thermocouple attached to the side of the gas cell. Because of the large thermal mass of the gas cell, it was necessary to stabilize the cell for 30 min at a given temperature so as to be certain equilibrium had been reached; then the infrared spectrum was recorded. Since the interior of the Beckman IR-11 unit was purged with dry nitrogen gas, no difficulty was encountered with frost or condensation

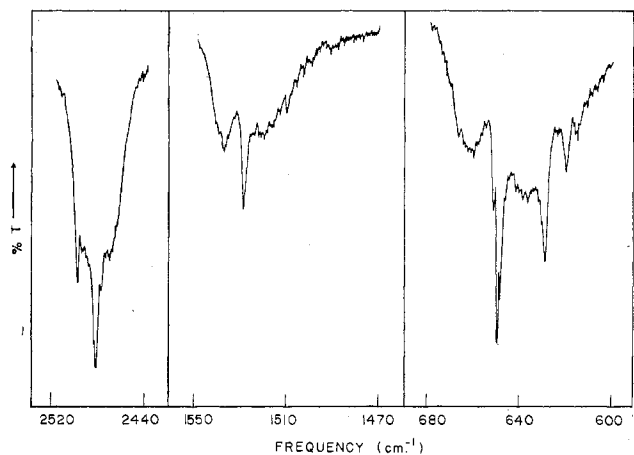


Figure 3.—Fine structure of medium-intensity infrared bands of HPF_4 : $p = 6.0$ cm, $l = 10$ cm, AgCl windows.

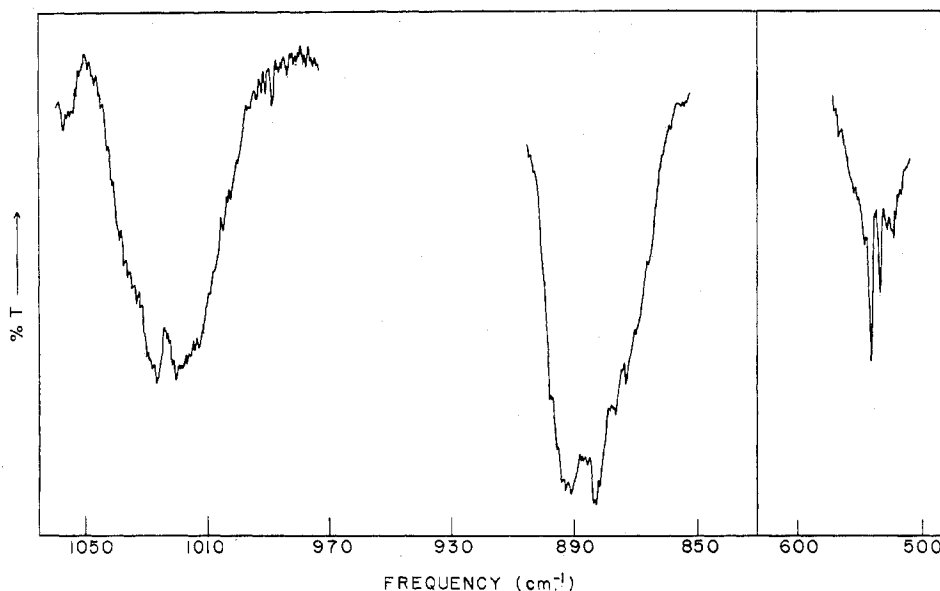


Figure 4.—Fine structure of strong infrared bands of HPF_4 : $p = 0.5, 0.25,$ and 0.5 cm, respectively, $l = 10$ cm, AgCl windows.

forming on the cell windows. Temperatures would be maintained well for periods long enough for accurate spectra to be run without difficulty.

Infrared spectra of frozen films were recorded in the range 200–2000 cm^{-1} with the use of a Sulfrin cryostat. The sample was deposited from the vapor on a CsI window precooled to 77°K. The sampling system consisted of all metal and Kel-F parts. The sample passed through a precision leak valve (Granville-Phillips Co., Boulder, Colo.) at a controlled rate. The deposition rate was varied in order to examine the quality of the resulting spectra. Full-scale spectra were obtained after deposition periods ranging from 0.5 to 4 hr with those obtained in the 2–3-hr periods having the best appearance.

By recovering the sample from the cold window after the spectral study, it was established by subsequent gas-phase infrared surveys that no decomposition and no changes in spectra took place for either HPF_4 or H_2PF_3 .

Raman displacements from the 6328-Å line of a Spectra-Physics Model 125 He–Ne laser were obtained with an instrument employing a Spex 1400 double-grating double monochromator containing 600 grooves/mm. Photon-counting electronics were activated by a FW 130 cathode photomultiplier having S-20 response.

In order to obtain low-temperature Raman spectra of the liquid and solid phases of HPF_4 and H_2PF_3 , a special sampling device was used. It consisted of a thin-walled Teflon sample tube which fitted snugly over a length of 1/8-in. copper tubing attached to a valve and standard taper for a vacuum connection. The entire

assembly was vacuum tight and withstood low temperatures without leaking. After condensation and isolation of the sample in the Teflon tube at liquid nitrogen temperature, the sample cell assembly was inserted into a precooled low-temperature accessory of the Harney–Miller type.¹¹ Use of the latter kept the sample controllably cooled down to -100° without allowing any condensation to form on the sample tube. The sample tube was supported by perforated Teflon spacers. By careful focusing of the laser beam, the Raman spectrum of Teflon could be virtually excluded from the spectrum of the sample. After completion of the recording of the Raman spectra, the samples were transferred into a gas-phase infrared cell and were surveyed. It was found that the infrared spectra were identical with those run prior to the Raman work for both H_2PF_3 and HPF_4 . No impurities were found to have formed, indicating good vacuum integrity of the Raman cell. Spectra were recorded in both polarization directions for the liquid state of HPF_4 and H_2PF_3 , and then the samples were refrozen to obtain the spectra for the solids.

Results

Infrared and Raman Spectra of HPF_4 .—The gas-phase infrared spectrum of HPF_4 is shown in Figure 1

(top), and the spectrum of the solid recorded at -190° is displayed in the lower portion. Figure 2 shows the Raman spectrum of HPF_4 in the liquid state. Details of gas-phase infrared band shapes are shown in Figures 3 and 4. The frequencies, relative intensities, states of polarization, and suggested assignments are summarized in Table I for the gas- and liquid-state spectra of HPF_4 .

For molecules of C_{2v} symmetry 11 infrared-active and 12 Raman-active fundamentals are expected with no degeneracies. Comparison of the data in Table I reveals that of the 11 liquid-state Raman bands associated with HPF_4 , seven have a counterpart in the gas-phase infrared spectrum with no unusual shifts in frequency going from the gas to the liquid states. Considering that HPF_4 is a relatively weak scatterer whose spectrum was obtained in a Teflon tube, the above correspondence provides reasonably good support that no pronounced change in structure is occurring between the two states. Detailed analysis based on the known² C_{2v} gas-phase structure bears out this contention.

(11) The low-temperature unit was constructed after a design by F. A. Miller and B. M. Harney, *Appl. Spectrosc.*, **24**, 291 (1970).

TABLE I
 VIBRATIONAL SPECTRUM OF HPF_4^a

Ir (gas) ^b		Band type	Raman (liq) ^c			Assignment, cm^{-1}
cm^{-1}	I		cm^{-1}	I	Pol	
Q	314	m	200	w	(dp)	$\nu_5(a_1)$
Q	320	m	(296)	vw	(dp)	$\nu_{12}(b_2)$
		(A, B)	336	w	(dp)	$\nu_6(a_2)$
			386	vw		$\nu_4\text{SiF}_4$
			478	w		$\nu_5\text{PF}_3$
	525	s				$\nu_4(a_1)$
Q	533.5	s	537	w	dp	$\nu_9(b_1)$
Q	541	s				
Q	614.5	m				
Q'	619.5	m	632	s	p	$\nu_3(a_1)$
Q	629	m				
P	637	m	(A, B)			$\nu_8(b_1)$
Q	650	m				
R	661	m	801	m	dp	$\nu_{11}(b_2)$
Q	790	w				
Q	801	w				
Q	882	vs	892	s	p	$\nu_2(a_1)$
R	892	vs				
Q	1020	vs	B			$\nu_7(b_1)$
Q	1027	vs				
Q	1087	vw				
	1205	vw				$2\nu_9 = 1082$ (A_1)
	1299	vw	1293	w	(dp)	$\nu_2 + \nu_{12} = 1202$ (B_2) $2\nu_8 = 1300$ (A_1)
Q	1373.5	m	1582	vw		$2\nu_{11} = 1602$ (A_1)
Q	1382	m				
P	1519	m				HPOF ₃ impurity
Q	1527.5	m	(A, B)			$\nu_{10}(b_2)$
R	1537	m				
	1682	vw				$\nu_7 + \nu_8 = 1677$ (A_1) $2\nu_8 + \nu_8 = 1799$ (B_1)
	1792	vw				$\nu_2 + \nu_7 = 1909$ (B_1) $\nu_2 + 2\nu_8 = 2182$ (A_1)
	1921	vw				
	2173	vw				
P	2470	m	2504	w	p	$\nu_1(a_1)$
Q	2481.5	m				
R	2501	m				
	2585 ^d	w	2586	vw	p	$2\nu_7 + \nu_4 = 2573$ (A_1)

^a p denotes polarized; dp, depolarized; sh, shoulder; br, broad; s, strong; m, medium; w, weak; v, very; (), uncertain. ^b Primes on Q indicate the presence of hot bands; otherwise, if more than one Q is listed, a split Q branch is inferred. ^c The liquid-state Raman spectrum was recorded with the sample at -63° . ^d Band head.

Further, no change in structure of any significance is apparent from examination of the liquid-state Raman spectrum (-63°) (Figure 2) and the solid-state Raman spectrum (-125°) discussed below. Other than a couple of the weaker intensity bands, all of the rest appear in the solid with approximately the same relative intensity and frequency as observed for the liquid. The only new feature is the appearance of a very weak line at 2552 cm^{-1} , possibly a combination of a lattice mode with a fundamental frequency or its overtone. A broad rise is observed peaking near 1140 cm^{-1} and is a typical occurrence resulting from fluorescence.

A similar relation exists between the gas-state and solid-state (Figure 1) infrared spectra. In the solid no bands above 1100 cm^{-1} were observed other than a weak absorption at 1430 cm^{-1} , not seen in the vapor.

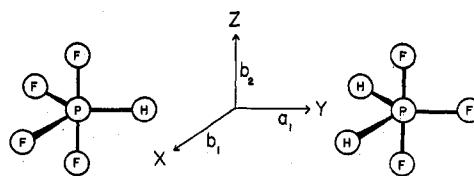


Figure 5.—Coordinates for HPF_4 and H_2PF_3 . The species a_1 , b_1 , and b_2 are shown associated with an appropriate coordinate axis.

This again may be some combination involving a lattice mode. The spectra below 1100 cm^{-1} are similar with sharper absorptions as expected in the solid.

There is an observed alteration on going to the solid in the relative intensities of the P-F stretching modes centered at 795 and 887 cm^{-1} in the vapor. As discussed below, the former is assigned to an asymmetric stretch and the latter to a symmetric stretch. It might be rationalized that solid-state effects are at play to reduce the magnitude of the dipole change for the symmetric mode relative to that for the asymmetric vibration. However, this point bears further study.

Feeling fairly confident that we are working with the same molecular conformation in the vapor and liquid states, assignment of the bands to appropriate species is aided largely by the polarization data, band shapes in the infrared, and region expected for particular modes to appear.

HPF_4 of C_{2v} symmetry is an asymmetric rotor. As such the three principal axes of rotation have different moments of inertia associated with them. With the coordinates as defined in Figure 5 and the parameters from Pierce and Cornwell,² the axis of greatest moment of inertia ($275.8 \times 10^{-40}\text{ g cm}^2$) is y , that of the intermediate moment ($184.9 \times 10^{-40}\text{ g cm}^2$), x , and the axis of least inertia ($141.2 \times 10^{-40}\text{ g cm}^2$), z . Based on the method of Badger and Zumwalt,¹² calculations show that vibrations of a_1 species (dipole change parallel to the y axis) will have C-type band shapes, those of b_1 species (dipole change parallel to the x axis) will have B-type band shapes, and b_2 species (dipole change parallel to the z axis) will have A-type contours.

Since the moments associated with the x and z axes are fairly close, C-type bands should differ more than A and B types, although A-type bands should have more intensity in the P and R branches while C-type bands would tend toward the opposite, concentrating more intensity in the Q branch under this approximation. Consequently, assignment of vibrations of a_1 species is aided by both polarization and band contour analysis in this instance.

There are three bands listed in Table I which are polarized and have sufficient intensity in the Raman to count as fundamentals. These are the 2504 cm^{-1} Raman band, assignable as the P-H stretch, and the two strong Raman displacements in the PF stretching region observed at 892 and 632 cm^{-1} . The higher of the two is associated with an equatorial stretch and the lower with an axial stretching mode in line with similar assignments on related molecules^{4,13} and the inherent weakness of axial compared to equatorial bonds.¹⁴

(12) R. M. Badger and L. R. Zumwalt, *J. Chem. Phys.*, **6**, 711 (1938).

(13) (a) J. E. Griffiths, R. P. Carter, Jr., and R. R. Holmes, *ibid.*, **41**, 863 (1964); (b) R. R. Holmes, *ibid.*, **46**, 3730 (1967).

(14) R. R. Holmes, *Accounts Chem. Res.*, **5**, 297 (1972).

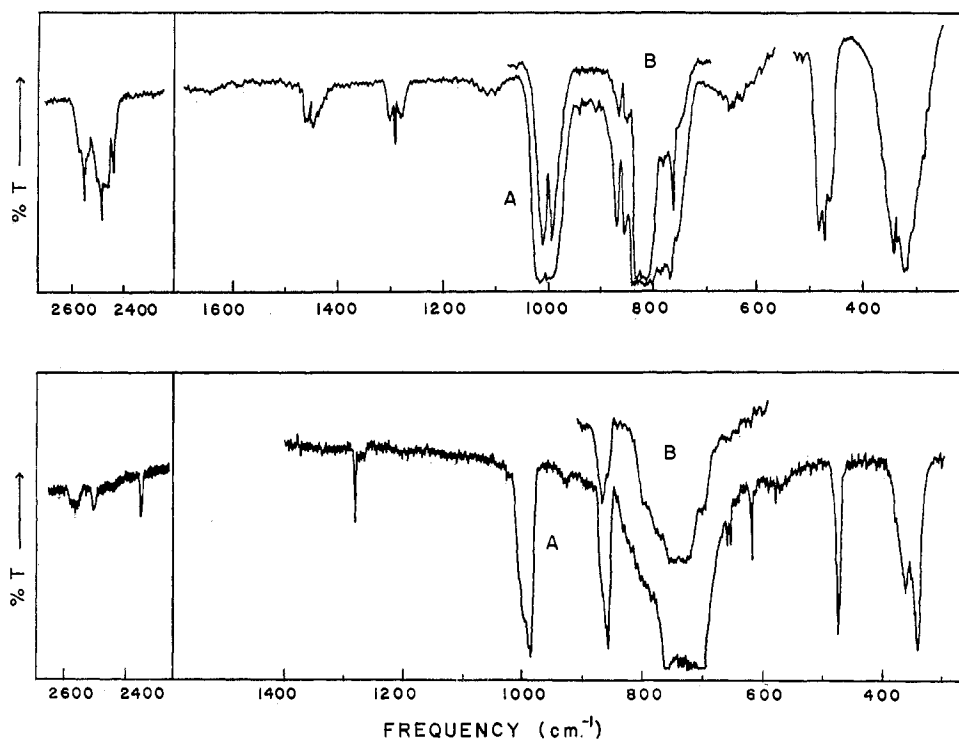


Figure 6.—Infrared spectrum of H_2PF_3 . Top, vapor at 25° : (A) $p = 3.5$ cm, (B) 1.0 cm; $l = 10$ cm, AgCl windows. Bottom, solid film: (A) thick film at -158° , (B) thin film at -190° ; CsI windows.

The infrared modes also appear to have C type band shapes. This is most clear for the 2481.5 cm^{-1} band shown in some detail in Figure 3. The composite band around 640 cm^{-1} (Figure 3) is thought to be two overlapping bands, one centered at 629 cm^{-1} , just discussed, showing "hot" bands to the low-frequency side and one centered at 650 cm^{-1} with typical PQR structure. The band contour for the 892 cm^{-1} band (Figure 4) resembles that for the 629 cm^{-1} band.

Two further bands serve as P-F stretches, the intense infrared band centered at 1024 cm^{-1} and the Raman band at 801 cm^{-1} of moderate intensity. The former band with no observable intensity in the Raman is assigned as the PF_2 asymmetric stretch (b_1 species) while the latter band having an infrared counterpart exhibiting a weak intensity is assigned, consistent with its lower frequency, to the remaining axial P-F stretch of b_2 species. The doublet Q branch for the infrared band centered at 1024 cm^{-1} is characteristic of a B-type band in agreement with the species designation.

The axial P-F bending vibrations usually appear^{4,13,15} around 500 cm^{-1} . Here as well, an absorption is found in this region in the infrared spectrum and a corresponding displacement in the Raman spectrum. In each spectrum, the band gives evidence of being a composite of two bands. In the infrared spectrum, we interpret the lower frequency component at 525 cm^{-1} as a C-type and a higher frequency component centered at 537 cm^{-1} with a doublet structure indicative of a B-type contour. These are assigned, respectively, as a_1 and b_1 species.

(15) (a) In view of recent electron diffraction amplitude data on trigonal-bipyramidal molecules of D_{3h} symmetry [L. S. Bartell, *Inorg. Chem.*, **9**, 1594 (1970)], it appears more consistent if the equatorial-in-plane and axial bending assignments¹³ are interchanged; (b) however, coupling is indicated between these two motions [R. R. Holmes and J. A. Colen, *ibid.*, **9**, 1596 (1970)].

An infrared band at 1527.5 cm^{-1} counts as a P-H bending vibration and is assigned to an out-of-plane bend rather than an in-plane bend based on electron diffraction data¹⁵ on related trigonal-bipyramidal molecules indicating a large degree of in-plane amplitude associated with a low-frequency bend compared to an out-of-plane amplitude. The in-plane fundamental is assigned to the infrared absorption appearing at 650 cm^{-1} , the only remaining unassigned band of high enough frequency for such a vibration. Neither of these bands has any observable intensity in the Raman spectrum which is not unexpected in view of the weakly appearing P-H stretch in the Raman region.

Again consistent with established assignments based on electron diffraction data^{15a} and vibrational interpretation,^{15b} the low-frequency mode at 200 cm^{-1} in the Raman is assigned as an equatorial in-plane PF_2 bend (a_1 species). The related frequency in PF_5 has been assigned¹⁶ at 174 cm^{-1} .

The only remaining infrared band unassigned, other than very weakly appearing combination modes observed at higher frequencies, is a band centered at 317 cm^{-1} . It has a weak counterpart in the Raman and is counted as a rocking vibration of b_2 species. A related mode which should be Raman active (a_2 species) and infrared inactive is assigned to the weak Raman feature at 336 cm^{-1} . This completes the spectral assignments in satisfactory agreement with the C_{2v} conformation shown by microwave spectroscopy.² Suggested assignments of combination and overtones for the very weakly appearing bands are listed in Table I.

Infrared and Raman Spectra of H_2PF_3 .—The infrared spectrum of H_2PF_3 in the gas state is shown in Figure 6 (top), and that for the solid in the lower por-

(16) F. A. Miller and R. J. Capwell, *Spectrochim. Acta, Part A*, **27**, 125 (1971).

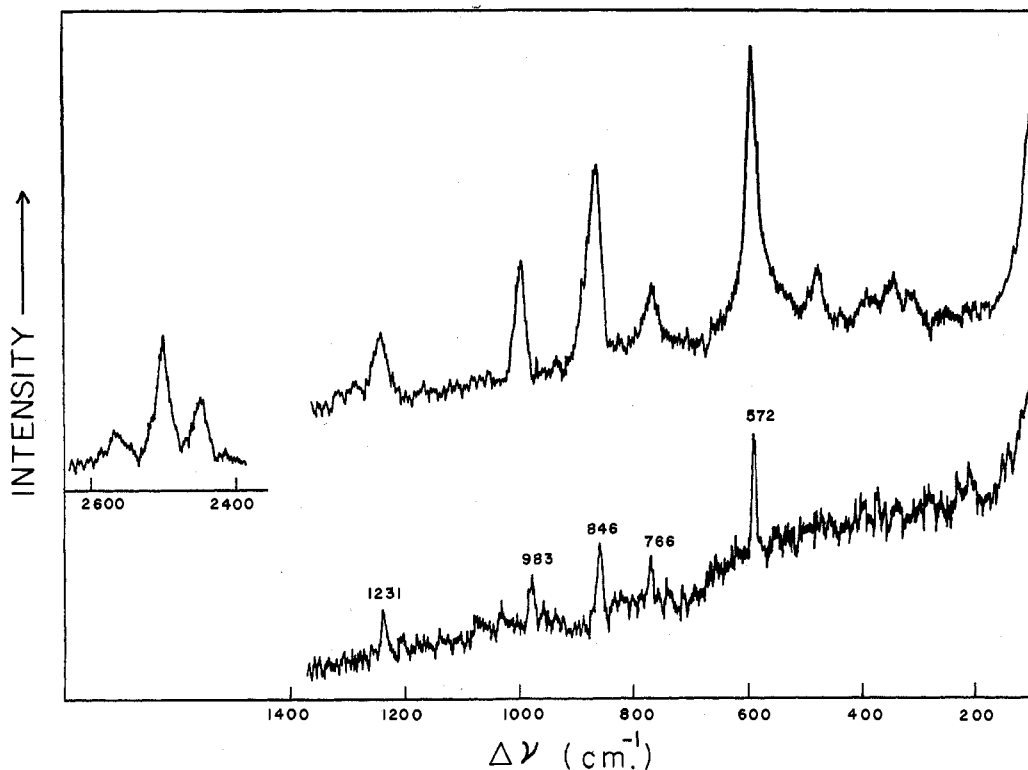


Figure 7.—Raman spectrum of H_2PF_3 : top, liquid at -28° ; bottom, solid at -157° .

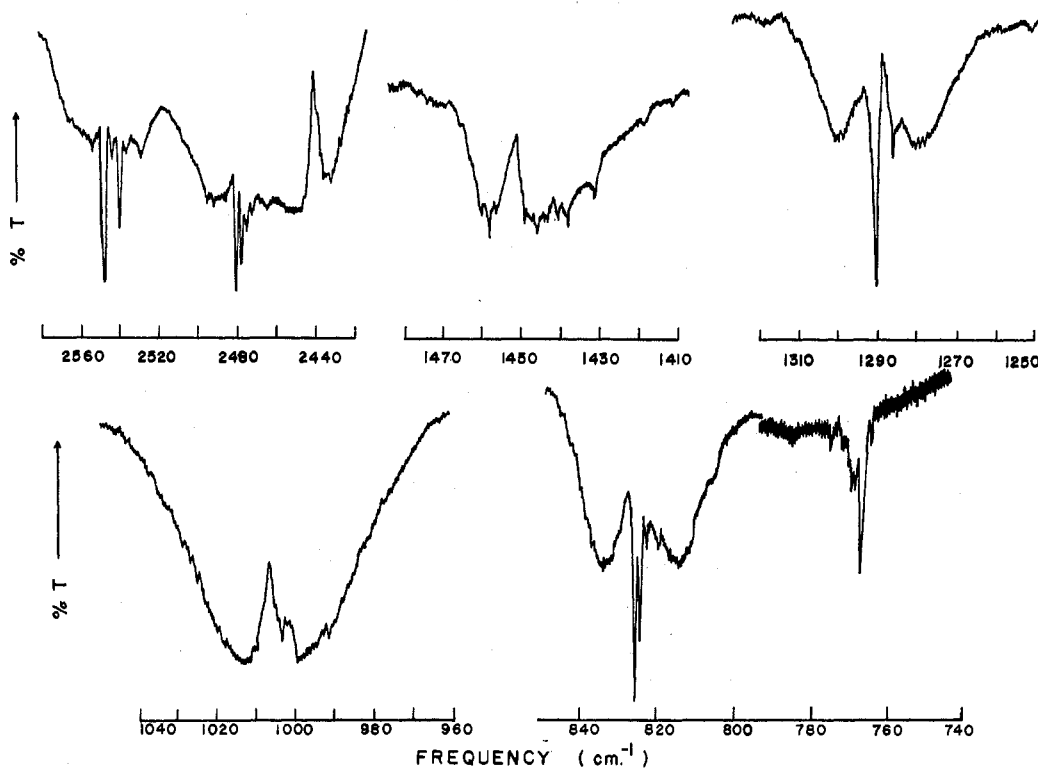


Figure 8.—Fine structure of infrared bands of H_2PF_3 : $p = 10.0$ cm for bands in the 1250 – 2600 - cm^{-1} region, $p = 0.7$ cm for the 1005 - cm^{-1} band, and $p \cong 0.2$ and 0.8 cm, respectively, for the lower frequency bands; $l = 10$ cm, AgCl windows.

tion. The liquid- and solid-state Raman spectra are presented in Figure 7. Details of gas-phase infrared band shapes are shown in Figures 8 and 9. Table II summarizes the pertinent vibrational data for H_2PF_3 with band assignments based on the C_{2v} symmetry for which arguments will be presented.

Comparison of the gas- and solid-state infrared spectra (Figure 6) reveals no startling differences. For the most part, the solid-state spectrum shows a similar distribution of intensities with slightly lowered frequencies in general compared to the gas-state spectrum. Only the weakest infrared bands are absent for the solid.

TABLE II
 VIBRATIONAL SPECTRUM OF H₂PF₃^c

Ir (solid) ^b		Ir (gas)		Band type	Raman (liq) ^c		Assignment, cm ⁻¹
cm ⁻¹	<i>I</i>	cm ⁻¹	<i>I</i>		cm ⁻¹	<i>I</i>	
					308	w (dp)	$\nu_{10} - \nu_8 = 286$ (B ₂)
		P 319	m				
		Q 335	m		336	w (dp)	ν_{12} (b ₂)
344	m	R 341	m				
365	m				377	w (dp)	ν_6 (a ₂)
		P 463.5	m				
		Q 472.5	m	C	472	w (dp)	ν_9 (b ₁)
474	m	R 483.0	m				
		P 587	w				
		Q 605	w		596	s p	ν_2 (a ₂)
620	w	Q 622	w				
		R 635	w				
		P (645)	w				
658	w	Q 659.5	w				
		Q 664	w				$2\nu_{12} = 670$
		R (674)	w				(A ₁)
		P 758	s				
720-765	vs, br	Q 767	s	C	766	w dp	ν_8 (b ₁)
		R 785	s				
		P 814	vs				
		Q'' 822	vs				
~800	s, sh	Q' 823.5	vs				
		Q 825	vs	A			ν_{11} (b ₂)
		R 833	vs				
		P 856	m				
860	m	R 871	m	B	879	s p	ν_4 (a ₁)
		P 998.5	vs				
984	s	R 1012	vs	B	996	m p	ν_3 (a ₁)
		P 1094	vw				
		Q 1104	vw				$\nu_5 + \nu_9 = 1094$ (B ₁)
		R 1117	vw		1233	w (dp)	ν_2 (a ₁)
		P 1280	w				
1277	w	Q 1291	w	A			ν_{10} (b ₂)
		R 1300	w				
		P 1445	w				$\nu_1 - \nu_3 = 1477$ (A ₁)
		R 1458	w	B			$2\nu_4 = 1728$ (A ₁)
		P 1718	vw				$\nu_8 + \nu_4 = 1869$ (A ₁)
		R 1734	vw				$2\nu_4 + \nu_{12} = 2063$ (B ₂)
		P 1856	vw				$3\nu_{11} = 2475$ (B ₂)
		R 1874	vw				
		2065	vw				
		P 2434	m				
2446	vw	R 2451	m	B	2444	vw p	ν_1 (a ₁)
		P 2467	m				
		Q' 2479	m				
		Q 2482	m		2499	w p	
2506	vw	R 2492	m				
2569	vw	2549 ^d	m		2564	vw p	ν_7 (b ₁)

^a p denotes polarized; dp, depolarized; sh, shoulder; br, broad; s, strong; m, medium; w, weak; v, very; (), uncertain. ^b Sample temperature, -158°. Primes on a Q branch indicate the presence of hot bands. Unprimed neighboring Q branches indicate a split Q band shape. ^c The sample temperature for the recording of the Raman spectrum was -28°. ^d Band head.

Intensity enhancement appears to occur in the solid for the strong gas-phase band listed at 767 cm⁻¹ relative to the very strong gas-phase band at 825 cm⁻¹. Resolution of the related solid-state band was not achieved, and it is reported as a very intense broad band centered at 745 cm⁻¹ with an apparent shoulder at about 800 cm⁻¹. The solid-state spectral frequencies observed at -158° are included in Table II for comparison with the vapor-state values. From the close spectral similarity between these two states, the basic structural entity is indicated to be the same in the gas and solid.

Also listed in Table II are the liquid-state Raman data determined at -28°. All the frequencies present have a counterpart in the infrared other than two weakly appearing bands at 1233 and 377 cm⁻¹. Further, the solid-state Raman spectrum determined at

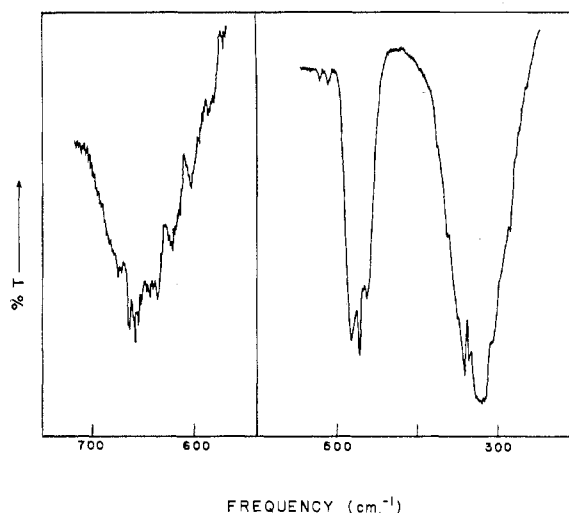


Figure 9.—Fine structure of low-frequency infrared bands of H₂PF₃: *p* = 50.0 cm for bands in the 575–700 cm⁻¹ region, AgCl windows; and *p* = 11.0 cm for bands in the 225–500-cm⁻¹ region, CsI windows, *l* = 10 cm.

-157° (a similar temperature as the solid-state infrared spectrum) shows (Figure 7) the same spectral pattern as that for the liquid Raman region but with somewhat reduced frequencies. A few of the weaker bands are absent in the Raman spectrum for the solid in line with its poorer scattering qualities, at least for the samples investigated. Again, no significant structural changes among the various states are indicated by these comparisons.

The trigonal bipyramid is the most likely structure for H₂PF₃, especially in view of the observance² of this form for HPF₄. However, the tetragonal pyramid is a possible alternative worth considering. For H₂PF₃ three trigonal bipyramids are possible, one of C_{2v} symmetry and the other two possessing D_{3h} and C_s symmetries. In the tetragonal pyramid, two C_s configurations with either one apical hydrogen atom or two adjacent basal hydrogens and one C_{2v} molecule with alternating hydrogen and fluorine atoms in the base are possibilities. Table III lists the fundamentals to be ex-

TABLE III
ACTIVITY OF FUNDAMENTAL MODES

Point group	Fundamentals	Raman	Ir	Coincidences
C _s	12	12 (8p)	12	12
C _{2v}	12	12 (5p)	11	11
D _{3h}	8	6 (2p)	5	3

pected and their activities for these symmetries.

Examination of Table II shows that of the 11 Raman bands that may reasonably be counted as fundamentals, four are polarized and eight have infrared counterparts. Eleven infrared vibrations serve as fundamentals. As a general structural indicator, the latter evaluation clearly rules out the D_{3h} symmetry. The C_s symmetry is unlikely by this count also since eight polarized bands are expected while the C_{2v} symmetry gives the best fit. The detailed analysis supplied below confirms these conclusions. Even so we are still left with two models having C_{2v} symmetry, one trigonal bipyramid and one square pyramid. Arguments will be presented in the discussion based on other evidence

leading to the rational choice of the trigonal bipyramid as the favored structure for H_2PF_3 . Accordingly, the assignments made here are for this model.

As with HPF_4 , the gas-phase infrared spectrum of H_2PF_3 shows highly structured bands (Figures 8 and 9) suggesting that band-shape analysis may be a significant aid in making assignments. Transferring the microwave parameters² for HPF_4 as an approximation for H_2PF_3 , moments of inertia are obtained. With reference to Figure 5, the axis of least moment of inertia (67.3×10^{-40} g cm²) is z , giving rise to A-type band contours for vibrations of b_2 species; the intermediate inertial axis, y (163.9×10^{-40} g cm²), gives rise to B-type contours associated with vibrations of a_1 species, the remaining axis, x , having the greatest moment (220.1×10^{-40} g cm²), gives C-type contours for vibrations whose dipole changes are parallel with this axis, b_1 .

Band shapes for b_2 vibrations (A type) are calculated¹² to have considerable intensity in the wings compared to b_1 vibration (C type). For vibrations of a_1 species (B type), a doublet structure might be revealed. Consistent with these calculations, examination of band shapes shown in Figures 8 and 9 shows three basic groups. Those vibrations which appear most amenable to this analysis have their shapes designated in Table II.

As with HPF_4 , the stretching frequencies are fairly easy to identify. The infrared (Figure 6) and Raman spectra (Figure 7) show three bands in the P-H stretching region with all three polarized. The latter is not expected and suggests coupling among these modes with a resultant transfer of intensity. Since two P-H stretches are expected, the lowest frequency band appearing on the shoulder of the infrared band centered at 2482 cm⁻¹ is assigned as an overtone of the most intense infrared band at 825 cm⁻¹. The higher of the two P-H stretches is listed as the asymmetric mode in Table II.

Two polarized bands of considerable intensity are present in the Raman spectrum in the region associated with P-F stretching vibrations. They are observed at 996 and 879 cm⁻¹ and have infrared counterparts. These are assigned, respectively, as the equatorial and axial stretch of a_1 species. The most intense band in the infrared at 825 cm⁻¹ with no corresponding Raman feature has a band shape indicating a b_2 vibration. It is reasonably expected that the asymmetric P-F axial stretch should appear as the most intense vibration for this molecule since the equatorial asymmetric stretch would involve a P-H motion to some extent having an accompanying low dipole change.

Two predominantly P-H bending vibrations are expected for C_{2v} symmetry, an equatorial-in-plane and an equatorial out-of-plane vibration. Three bands are observed in this region, two in the infrared spectrum and one in the Raman spectrum with no counterparts. However, the infrared absorption centered at 1451 cm⁻¹ in the vapor is absent in the infrared spectrum of the solid obtained at -157°. In view of this behavior, it is concluded that the latter frequency is a combination band, especially since all the other infrared bands counted as fundamentals in Table II have observable absorptions in the low-temperature solid-state spectrum. Because of the band shape for the in-

frared absorption at 1291 cm⁻¹, it is assigned to the out-of-plane bend of b_2 species while the Raman band at 1233 cm⁻¹ is associated with the in-plane motion of a_1 species.

Only one a_1 species remains unaccounted for, a P-F axial bend, and only one polarized Raman band remains unassigned. It is observed at 596 cm⁻¹ with a corresponding infrared absorption at 614 cm⁻¹. The P-F axial bending region, usually in the 450-550-cm⁻¹ range,^{4,13,15} might be expected to be somewhat higher here owing to some degree of interaction with equatorial P-H stretches.

Two infrared bands lying nearby at 472 and 767 cm⁻¹, both exhibiting band contours indicating b_1 species, serve as P-F bends. Both have related frequencies present in the Raman region showing depolarized bands. Since the equatorial-in-plane mode should have a greater participation by the hydrogen atoms than the mode associated with the axial bend, it is assigned the higher frequency in Table II.

The remaining modes to be assigned are rocking motions involving the molecule as a whole. One is infrared inactive for the symmetry considered and of a_2 species. This mode is assigned to the weak Raman displacement recorded at 377 cm⁻¹ with no infrared complement while the infrared absorption at 335 cm⁻¹ is taken as the other rocking vibration of b_2 species. It has a corresponding Raman frequency appearing weakly at 336 cm⁻¹, probably depolarized.

There are left only very weak bands in the infrared. These are counted as combination bands and given appropriate assignments in Table II. In addition, a weak band at 308 cm⁻¹ in the Raman spectrum is designated as a difference band. For comparison, the fundamental frequencies for H_2PF_3 and HPF_4 are summarized in Table IV along with mode descriptions.

TABLE IV
FUNDAMENTAL FREQUENCIES OF HPF_4 AND H_2PF_3

Mode description	HPF_4	H_2PF_3	CH_3PF_6^c
a_1			
PH stretch	2482	2482	725 (PC)
PF eq stretch	882	1005 ^b	932
PF_2' axial stretch	629	864 ^b	596
PF_2' axial bend	525	614 ^b	514 ^d
Eq in-plane bend	200 ^a	1233 ^a	179 ^d
a_2			
Rock	336 ^a	377 ^a	397
b_1			
Eq asym stretch	1024 ^b	2549 ^b	1009
Eq in-plane bend	650	767	179 ^d
PF_2' axial bend	537 ^b	472	467 ^d
b_2			
Eq out-of-plane bend	1528	1291	538
PF_2' axial asym. stretch	795 ^b	825	843
Rock	317 ^b	335	412

^a These are Raman frequencies. All others are gas-state infrared values. ^b Band centers. ^c Reference 23. ^d Reassignments, see text.

Discussion

Analysis of the vibrational data strongly suggests that the vapor-state structure of HPF_4 and H_2PF_3 is retained in the liquid and solid states. For HPF_4 this structure is a trigonal bipyramid of C_{2v} symmetry (Figure 5), previously established by microwave spec-

troscopy.² In the case of H_2PF_3 , Goubeau, *et al.*,⁹ concluded from a vibrational study that it was a similarly structured molecule of C_{2v} symmetry in the vapor state (Figure 5) but underwent association in the liquid and solid state to a preferred fluorine bridge dimeric unit. In contrast, our analysis shows that if any association is present, the resultant effect is insufficient to give rise to any new spectral bands in either the infrared or Raman regions in the condensed states.¹⁷

Goubeau, *et al.*,⁹ were led to a dimeric formulation based on the decidedly different solid-state infrared spectrum they observed compared to their vapor-state results. The latter are, in general, similar to ours, although two of their most intense bands at 389 and 1026 cm^{-1} , not present in our spectra (Table II), are most likely due to SiF_4 as a contaminant.

The absence of bands in the P-H stretching region in their solid-state infrared spectrum and the appearance of several new bands not present in the vapor, some admittedly doubtful in character, suggested to them that the rule of mutual exclusion was being followed and indicated a centrosymmetric structure. Their infrared data are shown in Table V for comparison with

TABLE V
INFRARED SPECTRUM OF GOUBEAU, *et al.*,⁹ FOR H_2PF_3

Gas		Solid	
Cm^{-1}	I	Cm^{-1}	I
3460	vw		
2960	vw		
2538	ms		
2465	m		
2240	m		
2060	vw		
1820	vw		
1452	w		
1325	m		
1292	m	1280	w
1190	w	1187	m
1148	w	1118	s
		1095	w
1026 ^b	vs		
995	s	960	s
		888	w
867	w		
820	vs		
765	m	713	vs
655	vw	481	vw? ^c
471	w	448	vw?
389 ^b	vs	329	vw?
329	vw	306	vw?
		286	vw?

^a Combination or overtone bands. ^b Most likely due to SiF_4 impurity. ^c The question marks are the authors' own designation.

ours in Table II.

We feel the lack of observance of P-H stretches is associated with the deposition of solid films of poor

(17) This does not preclude the possibility of a very weak association involving an unsymmetrical intermediate which could assist an intramolecular ligand exchange process. Some nmr evidence supporting mild association in the liquid was reported in ref 8, but some of the ambiguity in the results was resolved by later work on H_2PF_3 reported in ref 10. Similar to $(\text{CH}_3)_2\text{PF}_2$, A. J. Downs and R. Schmutzler, *Spectrochim. Acta, Part A*, **23**, 681 (1967), the asymmetric PF axial stretch for H_2PF_3 shows a pronounced downfield shift in the condensed state relative to the vapor suggestive of mild association.

quality. Some evidence for this is seen by comparing our solid-state spectrum in Figure 6 below 700 cm^{-1} showing relatively sharp bands of medium to weak intensity in contrast to the very weak features listed in Table V. The strong band reported⁹ at 960 cm^{-1} in Table V is clearly seen at 984 cm^{-1} in Figure 6, while the difference in frequency between the most intense band in the solid state they report⁹ at 713 cm^{-1} and we observe in the 720–765- cm^{-1} region is again most likely a function of the conditions of sample preparation. With fast deposition rates (~ 0.5 hr), a skewed appearance is obtained for this band, indicating a lower frequency.

For several of the frozen films we prepared, the sample temperature was raised to about -100° to allow possible structural rearrangement to occur. No changes in the infrared spectrum took place following this treatment.

The retention of one structural representation for H_2PF_3 on going from the gas to the condensed state is consistent with ^{19}F nmr data¹⁰ discussed in the Introduction. The fact that P-F spin coupling is retained on warming H_2PF_3 from -46° (where two fluorine atom environments are indicated¹⁰ in the ratio of 2:1) to -15° (where one fluorine atom environment is seen) argues against the formation of a symmetrical dimeric species in the liquid but is consistent with the onset of ligand exchange proceeding by an intramolecular exchange mechanism. The latter nmr behavior is typical of molecules of the class Y_2PF_3 ,^{14,18,19} such as $(\text{CH}_3)_2\text{PF}_3$ ³ and Cl_2PF_3 ,¹⁹ where structures have been rather clearly established. In this respect, while the infrared and Raman data reported here show H_2PF_3 to have C_{2v} symmetry, as pointed out in the analysis section above, the data do not distinguish between the trigonal bipyramid with equatorially positioned protons and a square pyramid having an axial fluorine atom and alternating fluorine and hydrogen atoms in the basal positions. However, the trigonal bipyramid is strongly favored by analogy with the known structure for HPF_4 ² as well as that for other molecules of the class Y_2PF_3 .^{3,14,19}

Additionally, both simple repulsion arguments^{14,20} and molecular orbital calculations²¹ show that the trigonal bipyramid is favored in that less electronegative ligands are expected to occupy the axial position of a square-pyramidal structure for phosphorus compounds in contrast to that which would result for the C_{2v} square pyramid for H_2PF_3 .

Regarding the specific exchange mechanism, as with other molecules of this class,¹⁴ normal coordinate calculations suggest that the largest amplitude bending motions are of b_1 symmetry and indicate a path of the type $\text{I} \rightleftharpoons \text{II}$.

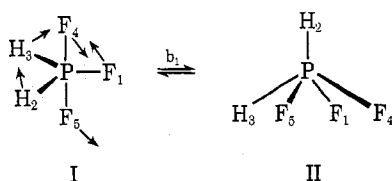
For HPF_4 the lowest frequency bending motions (Table IV) and largest amplitudes are of a_1 species sug-

(18) (a) E. L. Muetterties, W. Mahler, and R. Schmutzler, *Inorg. Chem.*, **2**, 613 (1963); (b) E. L. Muetterties, W. Mahler, K. J. Packer, and R. Schmutzler, *ibid.*, **3**, 1298 (1964); (c) R. Schmutzler, *Angew. Chem., Int. Ed. Engl.*, **4**, 496 (1965).

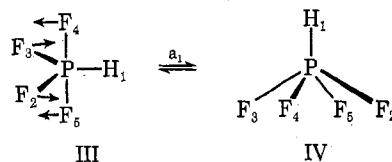
(19) R. R. Holmes, R. P. Carter, Jr., and G. E. Peterson, *Inorg. Chem.*, **3**, 1748 (1964).

(20) (a) R. J. Gillespie, *Can. J. Chem.*, **38**, 818 (1960); (b) R. J. Gillespie, *J. Chem. Educ.*, **40**, 295 (1963).

(21) A. Rauk, L. C. Allen, and K. Mislow, *J. Amer. Chem. Soc.*, **94**, 3035 (1972).



gesting that intramolecular ligand exchange indicated by nmr data proceeds *via* the Berry process.^{14,22}



Finally, the normal mode descriptions for HPF_4 and H_2PF_3 are compared with those for CH_3PF_4 in Table IV. The initial frequency assignments by Downs and Schmutzler⁷ for CH_3PF_4 have been altered in Table IV. In line with the potential field refinement²³ resulting from electron diffraction work on more symmetric trig-

(22) R. S. Berry, *J. Chem. Phys.*, **32**, 933 (1960).

(23) (a) L. S. Bartell, *Inorg. Chem.*, **9**, 1594 (1970); (b) R. R. Holmes and J. A. Golen, *ibid.*, **9**, 1596 (1970).

onal bipyramids including CH_3PF_4 , a lower frequency associated with an equatorial relative to an axial bending mode is suggested. Consequently, assignments of the corresponding modes for both the a_1 and b_1 species of CH_3PF_4 have been interchanged compared to the original²³ mode designations. On this basis, the tabulated frequencies compare favorably between HPF_4 and CH_3PF_4 . The effect of the introduction of the proton relative to the methyl group is seen as an increase in frequency of the equatorial in-plane and equatorial out-of-plane bend of b_1 and b_2 species, respectively.

Relative to HPF_4 , both the equatorial and axial PF stretches of a_1 species of H_2PF_3 are at a considerably higher frequency and suggests a mode description for H_2PF_3 containing a greater degree of mixing with the PH stretching coordinate of the same species. The latter seems reasonable for the more highly protonated fluoride. A comparison of frequency assignments for related molecules has been given elsewhere.²⁴

Acknowledgment.—Grateful appreciation is expressed for support of this work by a grant from the National Science Foundation. We also wish to thank Dr. Robert Larkin for assistance in obtaining the laser Raman spectra.

(24) R. R. Holmes and M. Fild, *J. Chem. Phys.*, **53**, 4161 (1970).

CONTRIBUTION FROM THE DEPARTMENT OF CHEMISTRY,
VANDERBILT UNIVERSITY, NASHVILLE, TENNESSEE 37235

Synthesis of the Two Isomeric N-Methyl-1,2,4,6,3,5-thia(VI)triazadiphosphorines

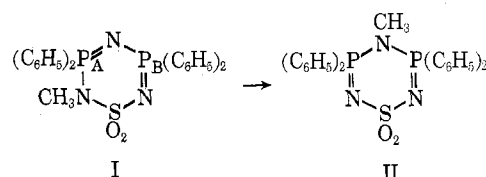
By MANFRED BERMANN¹ AND JOHN R. VAN WAZER*

Received January 20, 1972

The two isomers corresponding to a methyl group being positioned at the N' and N'' atoms in the cyclic molecule $\text{S}(\text{O}_2)\text{N}'\text{P}(\text{C}_6\text{H}_5)_2\text{N}''\text{P}(\text{C}_6\text{H}_5)_2\text{N}$ have been prepared by ring-closure reactions. The compound having the methyl group on the N' was obtained from iminobis(chlorodiphenylphosphonium) chloride and N,N' -dimethylsulfamide or by metathesis from iminobis(methylaminodiphenylphosphonium) chloride and sulfur chloride. The other compound, with the methyl group on the N'' , was synthesized from bis(chlorodiphenylphosphazo) sulfone and heptamethyldisilazane. ^1H and ^{31}P nmr spectra as well as ir spectra are utilized as structure proofs.

Introduction

Several six-membered ring systems, containing phosphorus, nitrogen, and sulfur are known.^{2,3} Since only a few compounds with an endocyclic sequence $\text{S}-\text{N}-\text{P}-\text{N}-\text{P}-\text{N}$ have been prepared,⁴⁻⁷ the possibility of obtaining isomers of the forms I and II by specific ring-closure reactions seemed worthy of attention and constitutes the scope of the present work.



Experimental Section

Materials.—All solvents used were Spectrograde quality and practically water free. Sulfamide (Alfa) was used as received. Practical grade sulfur chloride was redistilled before use and the fraction boiling at 69–70° (757 Torr) retained. Methylamine (Matheson) was dried by passage over KOH pellets. The other starting compounds, *i.e.*, N,N' -dimethylsulfamide,⁸ iminobis(chlorodiphenylphosphonium) chloride,⁹ $[(\text{C}_6\text{H}_5)_2\text{P}(\text{Cl})_2\text{N}^+\text{Cl}^-]$ (III), and heptamethyldisilazane¹⁰ were prepared according to the literature. Diphenyltrichlorophosphorane is best prepared as given below.

(8) M. Bermann and J. R. Van Wazer, submitted for publication in *Synthesis*.

(9) E. Fluck and F. L. Goldmann, *Chem. Ber.*, **96**, 3091 (1963).

(10) R. C. Osthoff and S. W. Kantor, *Inorg. Syn.*, **5**, 58 (1957).

(1) Postdoctoral Research Fellow, 1970–1972.

(2) S. Pantel and M. Becke-Goehring, "Sechs- und achtgliedrige Ring-systeme in der Phosphor-Stickstoff-Chemie," Springer-Verlag, Berlin, Heidelberg, New York, 1969, p 259 ff.

(3) I. Haiduc, "The Chemistry of Inorganic Ring Systems," Vol. II, Wiley-Interscience, London, New York, Sydney, Toronto, 1970, p 813 ff.

(4) M. Becke-Goehring, K. Bayer, and T. Mann, *Z. Anorg. Allg. Chem.*, **346**, 143 (1966).

(5) R. Appel, D. Hännsgen, and B. Ross, *Z. Naturforsch. B*, **22**, 1354 (1967).

(6) U. Bieller and M. Becke-Goehring, *Z. Anorg. Allg. Chem.*, **380**, 314 (1971).

(7) U. Klingebiel and O. Glemser, *Chem. Ber.*, **104**, 3804 (1971).